Antimicrobial Peptides Derived from the Immune Defense Protein CAP37 Inhibit TLR4 Activation by S100A9

Anne Kasus-Jacobi,[1–3] Craig A. Land,[1] Amanda J. Stock,[1,*] Jennifer L. Washburn,[1] and H. Anne Pereira[1,3–5]

[1]Department of Pharmaceutical Sciences, University of Oklahoma Health Sciences Center, Oklahoma City, Oklahoma, United States
[2]Department of Physiology, University of Oklahoma Health Sciences Center, Oklahoma City, Oklahoma, United States
[3]Oklahoma Center for Neuroscience, University of Oklahoma Health Sciences Center, Oklahoma City, Oklahoma, United States
[4]Department of Pathology, University of Oklahoma Health Sciences Center, Oklahoma City, Oklahoma, United States
[5]Department of Cell Biology, University of Oklahoma Health Sciences Center, Oklahoma City, Oklahoma, United States

Correspondence: Anne Kasus-Jacobi, University of Oklahoma Health Sciences Center, 1110 N. Stonewall Avenue, Oklahoma City, OK 73117-1223, USA; anne-kasus-jacobi@ouhsc.edu.

Current affiliation: *National Institute on Aging, National Institutes of Health, Baltimore, Maryland, United States.

Received: November 19, 2019
Accepted: February 14, 2020
Published: April 16, 2020

Citation: Kasus-Jacobi A, Land CA, Stock AJ, Washburn JL, Pereira HA. Antimicrobial peptides derived from the immune defense protein CAP37 inhibit TLR4 activation by S100A9. *Invest Ophthalmol Vis Sci.* 2020;61(4):16. https://doi.org/10.1167/iovs.61.4.16

Purpose. Corneal abrasion is a common eye injury, and its resolution can be seriously complicated by bacterial infection. We showed that topical application of the cationic antimicrobial protein of 37 kDa (CAP37) promotes corneal re-epithelialization in mice, and peptides derived from CAP37 can recapitulate the antibacterial and wound-healing effects of the full-length protein. The current study was designed to identify the molecular mechanisms mediating the wound-healing effect of CAP37 and derived bioactive peptides.

Methods. We used a TriCEPS-based, ligand-receptor glycocapture method to identify the binding partners of CAP37 on live human corneal epithelial cells using the hTCEpi cell line. We used an ELISA method to confirm binding with identified partners and test the binding with CAP37-derived peptides. We used a reporter cell line to measure activation of the identified membrane receptor by CAP37 and derived peptides.

Results. We pulled down S100 calcium-binding protein A9 (S100A9) as a binding partner of CAP37 and found that CAP37 and four derived peptides encompassing two regions of CAP37 bind S100A9 with high affinities. We found that CAP37 and the S100A9-binding peptides could also directly interact with the Toll-like receptor 4 (TLR4), a known receptor for S100A9. CAP37 and one peptide partially activated TLR4. The other three peptides did not activate TLR4. Finally, we found that CAP37 and all four peptides could inhibit the activation of TLR4 by S100A9.

Conclusions. This study identifies a mechanism of action for CAP37 and derived antimicrobial peptides that may restrain inflammatory responses to corneal injury and favor corneal re-epithelialization.

Keywords: neutrophil granule protein, damage-associated molecular pattern molecule, pattern recognition receptor, corneal wound healing

Corneal abrasion of the epithelium is one of the most common eye injuries.[1,2] It is usually caused by a mechanical scratch from direct contact with particles (e.g., dust, sand, wood). It is also often caused by extended-wear contact lenses.[1,2] Corneal abrasion is painful, but in most cases it is not a serious condition because re-epithelialization occurs quickly and spontaneously.[1,2] However, a serious risk associated with corneal abrasion is infection due to bacterial or fungal pathogens invading the tissue through the breach created by the abraded epithelium.[2,3] Any delay in corneal re-epithelialization increases the risk for corneal infection and complications such as scarring, melting, and perforation. Such delays can be due to the use of topical anesthetics, antibiotics, antifungals, or steroids[4] and are common in patients with persistent corneal epithelial defects.[5]

The cationic antimicrobial protein of 37 kDa (CAP37), also called azurocidin, belongs to the innate immune system and has a protective role in the cornea.[6] CAP37 was first identified as a component of polymorphonuclear neutrophils.[7] It is prepackaged in the azurophil and secretory granules of neutrophils and is released upon infiltration and activation of these cells during tissue infection and inflammation.[7] Following corneal abrasion, neutrophils infiltrate the corneal stroma. In a mouse model of corneal abrasion, an early wave of neutrophil infiltration, peaking at 12 to 18 hours post-injury, appears to be essential

for re-epithelialization.[8] In addition to being constitutively expressed in neutrophils, CAP37 was found to be induced in the corneal epithelium following induction of bacterial keratitis in rabbits.[9] Positive staining for CAP37 in the corneal epithelium was observed as early as 5 hours post-infection, indicating that CAP37 could contribute to early defense mechanisms at the ocular surface.[9]

We tested the effects of topical administration of CAP37 in a mouse model of corneal abrasion and found that CAP37 promoted corneal re-epithelialization.[6] At the cellular level, corneal epithelial wound healing consists of migration, proliferation, and reattachment of the corneal epithelial cells to the basement membrane.[3,4,10] Migration and proliferation of cultured human corneal epithelial cells were significantly induced by CAP37.[11,12] The adhesion molecules $\alpha 3$ and $\beta 1$ of the integrin family were also upregulated in cultured human corneal epithelial cells upon treatment with CAP37.[11] This could favor reattachment of the corneal epithelial cells to the basement membrane, because the heterodimer $\alpha 3\beta 1$ constitutes the receptor for fibronectin, laminin 5, and laminin 10, which are major components of the corneal basement membrane.[11] These results demonstrated that CAP37 has direct effects on human corneal epithelial cells, promoting the three phases of corneal re-epithelialization.[11] At the molecular level, we hypothesized that these effects were mediated by transmembrane receptors of CAP37, expressed in corneal epithelial cells. These receptors are unidentified but our previous studies suggested a possible engagement of a G-protein-coupled receptor (GPCR) and of protein kinase C delta (PKCδ) for the migration of human corneal epithelial cells[12] and for corneal re-epithelialization[6] induced by CAP37.

In recent years, our goal has been to generate peptides that mimic the antimicrobial and wound-healing properties of full-length CAP37 for therapeutic purposes. Structure–function studies reviewed in Griffith et al.[3] identified three bioactive peptides derived from CAP37. Briefly, native and modified peptides derived from residues 20 to 44 of CAP37 are antimicrobial; a peptide covering the 95 to 122 region of CAP37 is not antimicrobial but can induce human corneal epithelial cell migration and enhance corneal re-epithelialization in mice; and, finally, a modified peptide derived from residues 120 to 146 of CAP37 is particularly interesting because it carries both functions.[3,13] These peptides could be beneficial to promote corneal re-epithelialization and thus minimize the risk of infection or other vision-threatening consequences of corneal abrasion.

The current study was designed to investigate the molecular mechanisms mediating the effects of CAP37 on human corneal epithelial cells and to determine whether the bioactive CAP37-derived peptides can activate the same molecular mechanisms. In this paper, we describe the binding of CAP37 and certain derived peptides to Toll-like receptor 4 (TLR4) and its agonist, S100 calcium-binding protein A9 (S100A9), and the effect of such binding on TLR4 activation.

Materials and Methods

Materials

The LRC-TriCEPS-CaptiRec kit (P05201) was purchased from Dualsystems Biotech AG (Schlieren, Switzerland). CAP37 (Azurocidin, 16-14-012621), neutrophil elastase (NE, 16-14-051200), and cathepsin G (CG, 16-14-030107), purified from human neutrophils, were purchased from Athens Research and Technology (Athens, GA, USA). Lipopolysaccharides from *Escherichia coli* 0111:B4 (L2630) and BSA (A3803) were obtained from Sigma-Aldrich (St. Louis, MO, USA). Recombinant human S100 calcium binding proteins S100A8 (untagged, pro-800) and S100A9 (fused to a C-terminus 8-His tag, pro-814) were purchased from Prospec Protein Specialists (Ness Ziona, Israel). Recombinant human TLR4/myeloid differentiation factor 2 (MD-2) complex (both proteins fused to a C-terminus 10-His tag, 3146-TM-050) was purchased from R&D Systems (Minneapolis, MN, USA). CAP37-derived peptides, spanning residues 20 to 44, 95 to 122, and 120 to 146 of the protein, were synthesized by CSBio (Menlo Park, CA, USA) with a purity of ≥95%, as previously described.[13] Peptide analogs 120 to 146 WH used in this study were modified from the native sequence of CAP37 (120-146 QR). The native residues Q and R in positions 131 and 132 were substituted by W and H, respectively. To optimize large-scale production and solubility of the bioactive peptides, five arginine (R) residues and two miniPEG (MP) moieties were added to each peptide, and the resulting modified peptides were 20-44 5RMP, 95-122 5RMP, and 120-146 WH 5RMP. The human corneal epithelial cell line human telomerase-immortalized corneal epithelial cell line (hTCEpi), immortalized by infection with human telomerase reverse transcriptase, was obtained from James V. Jester (University of Texas Southwestern Medical Center, Dallas, TX, USA). The human TLR4 reporter cell line HEK-Blue hTLR4 (hkb-htlr4) was derived from HEK-293 cells, co-transfected with the human *TLR4* gene, *MD*-2 and *CD14* co-receptor genes, and the secreted alkaline phosphatase (*SEAP*) reporter gene. These cells were purchased from InvivoGen (San Diego, CA, USA).

TriCEPS-Based Capture of Interacting Glycoproteins

The glycoprotein capture experiment was carried out using purified human CAP37 as the ligand. The core component of the LRC-TriCEPS-CaptiRec kit used for this experiment is the TriCEPS reagent. It contains three functional groups: (1) an NHS ester for conjugating TriCEPS to primary amine group-containing ligands, (2) a hydrazide group for the ligand-based capture of glycosylated proteins expressed by living cells, and (3) a biotin tag for purifying captured glycosylated proteins for analysis by quantitative mass spectrometry. TriCEPS was first coupled to CAP37 and to insulin, provided in the LRC-TriCEPS-CaptiRec kit. The latter was used as a control. Each protein (300 µg) was dissolved in 150 µl of HEPES buffer (25 mM, pH 8.2). Then, 1.5 µl of TriCEPS reagent was added to each sample, and samples were incubated for 90 minutes at 20°C under gentle agitation.

We next carried out the glycoprotein capture step, using 10^8 hTCEpi cells for each reaction. Cells were grown to confluence in large square bioassay dishes (500 cm^2 growth area; Corning Inc., Corning, NY, USA) in defined keratinocyte serum-free medium (Gibco, Grand Island, NY, USA) supplemented with growth factors provided by the manufacturer. L-Glutamine (2 mM; Gibco) and antibiotic-antimycotic (0.1 units/mL penicillin G sodium, 100 µg/mL streptomycin sulfate, 0.25 µg/mL amphotericin B; Gibco) were also added to the complete growth medium. Cells were mildly oxidized so that the second arm of TriCEPS would bind covalently to the glycans of the target proteins. To mildly oxidize cell surface proteins, the growth medium

was removed and replaced with 15 ml of oxidation solution (1.5-mM sodium metaperiodate in PBS, pH 6.5, containing 1% fetal bovine serum [FBS]) and incubated for 15 minutes at 4°C in the dark under gentle agitation. Oxidation solution was then removed and replaced with 10 ml TriCEPS-bound ligand solution (prepared by mixing 150 µl of TriCEPS-bound CAP37 or TriCEPS-bound insulin with 180 ml PBS, pH 6.5, containing 1% FBS), and incubated for 90 minutes at 4°C in the dark under gentle agitation. The ligand-containing buffer was removed, and cells were detached using 25 ml citrate saline buffer (135-mM potassium chloride, 15-mM sodium citrate) per dish and incubated for 120 minutes at 37°C. Most of the cells were detached from the plates by pipetting up and down after incubation with the citrate saline buffer. Cells that remained attached to the plates were gently scraped. Cells from eight plates were pooled together and centrifuged to generate a single cell pellet containing approximately 10^8 cells. Three pellets of cells that were incubated with the CAP37 ligand and three pellets of cells that were incubated with the insulin control ligand were washed once with PBS (pH 6.5) containing 1% FBS and then centrifuged again. All six resulting cell pellets were frozen and shipped to Dualsystems Biotech AG for analysis and identification of interacting proteins.

Liquid Chromatography with Tandem Mass Spectrometry Analysis

Upon receipt of the frozen pellets, Dualsystems Biotech AG performed cell lysis, protein purification, tryptic digestion, and mass spectrometric analysis of samples on a Thermo LTQ Orbitrapt XL spectrometer (Thermo Fisher Scientific, Waltham, MA, USA) fitted with an electrospray ion source, as described previously.[14] Peptide identifications were filtered to a false-discovery rate of ≤1% and quantified using an MS1-based label-free approach. For the MS1 quantification, we used the Nonlinear Dynamics Progenesis QI for proteomics (Durham, NC, USA). Protein identification relying on only one peptide has not been considered for such analysis. The six individual samples were analyzed with a statistical ANOVA model. This model assumes that the measurement error follows a Gaussian distribution, views individual features as replicates of a protein's abundance, and explicitly accounts for this redundancy. It tests each protein for differential abundance in all pairwise comparisons of ligand and control samples and reports the *P* values. Next, *P* values were adjusted for multiple comparisons to control for the experiment-wide false discovery rate (FDR). The adjusted *P* value obtained for every protein was plotted against the magnitude of the fold-enrichment between the two experimental conditions. The area in the volcano plot that showed an enrichment factor of 4 or greater and an FDR-adjusted *P* value of less than 0.01 was defined as the protein candidate space.

Enzyme-Linked Immunosorbent Assay

To confirm direct interaction of CAP37 with candidate binding partners, we conducted ELISA experiments, as described before.[15] Briefly, Nunc Maxisorp plates (Thermo Fisher Scientific) were coated with 5 µg/ml of BSA, CAP37, NE, CG, lipopolysaccharide (LPS), or CAP37-derived peptides dissolved in PBS (pH 7.4) for 2 hours at room temperature with shaking and then placed at 4°C overnight. After coating, plates were washed with PBST (0.05% Tween 20 in PBS, v/v; Sigma-Aldrich) and blocked with 3% BSA in PBST (w/v) for 1 hour at room temperature. Next, plates were washed again, and His-tagged S100A9 or His-tagged TLR4/MD-2 antigen, prepared in PBST 0.1% BSA, was added at concentrations ranging from 0 to 100 nM. Plates were incubated with antigens at 37°C for 70 minutes and washed, and mouse monoclonal anti-His tag primary antibody (Abcam, Cambridge, MA, USA) prepared in PBST with 1% BSA was added at concentrations of 0.5 µg/ml for S100A9 and 1.0 µg/ml for TLR4/MD-2. Plates were incubated at room temperature for one hour and then washed. Next, the secondary antibody peroxidase-conjugated AffiniPure Donkey Anti-Mouse IgG (Jackson ImmunoResearch Laboratories, West Grove, PA, USA) prepared in PBST was added at a concentration of 0.08 µg/ml and incubated at room temperature for 1 hour. Following incubation with the secondary antibody, plates were washed, and 100 µl of citrate buffer was added to the wells and allowed to develop for 10 to 30 minutes in the dark. After development, reactions were stopped using 50 µl of 5-N sulfuric acid (J.T. Baker Chemical Co., Phillipsburg, NJ, USA), and optical density (OD) values were recorded at 492 nm using a Synergy2 microplate reader and Gen5 1.11.5 software (BioTek Instruments, Inc., Winooski, VT, USA).

HEK-Blue hTLR4 Cell Culture and Stimulation Assay

HEK-Blue hTLR4 cells were cultured in complete growth medium: phenol red-free DMEM high glucose medium (Gibco) supplemented with 55-nM sodium pyruvate (Sigma-Aldrich), 10% heat-inactivated FBS (Gibco), 50 U/ml penicillin, 50 µg/ml streptomycin (Lonza, Walkersville, MD, USA), 2-mM L-glutamine (Gibco), 100 µg/ml Normocin (InvivoGen), and 1X HEK-Blue Selection (InvivoGen). All stimulation assays were performed on cells at passages between 3 and 15. To prepare cells for stimulation assays without detaching them from the plate, they were carefully rinsed once with ice-cold PBS to remove residual FBS. Then, 5 ml of pre-warmed PBS was added and dishes were incubated at 37°C for 2 minutes to promote cell detachment. Cells were fully detached from plates with gentle tapping, collected, and centrifuged at 52*g* for 5 minutes. Cell pellets were resuspended in complete growth medium without FBS at a final concentration of 1.4×10^5 cells/ml and immediately used for stimulation assays.

To quantify the activation of TLR4 in HEK-Blue hTLR4 cells, experimental treatments with protein or peptide ligands were prepared in nuclease-free water (Ambion, Thermo Fisher Scientific), using protein LoBind tubes (Eppendorf, Hamburg, Germany) and low-binding tips (Sorenson BioScience, Inc., Murray, UT, USA). First, 20 µl of experimental treatments were added in duplicate or triplicate to a flat-bottom, 96-well plate (Falcon, Durham, NC, USA). Then, 180 µl of the cell suspension prepared at 1.4×10^5 cells/ml was immediately added, and the plate was incubated for 24 hours at 37°C under 5% CO_2. Secreted alkaline phosphatase (SEAP) production was measured in each challenged well by transferring 20 µl of medium to a fresh 96-well plate containing 200 µl of pre-warmed Quanti-Blue detection medium (InvivoGen). The *SEAP* reporter gene is under the control of an IL-12 p40 minimal promoter fused to five nuclear factor kappa B (NF-κB) and activator protein 1 (AP-1) binding sites. Stimulation of these cells by

Investigative Ophthalmology & Visual Science

TLR4 ligands activates NF-κB, which in turn stimulates SEAP production. The Quanti-Blue plate was developed at 37°C, 5% CO_2, for 3 hours followed by OD recordings at 630 nm using the Synergy2 microplate reader and Gen5 software. In order to normalize the results of each well to the number of cells, 20 µl of 10% Triton X-100 Surfact-Amps Detergent Solution (Thermo Fisher Scientific) was added to the wells of the challenged plate. The plate was placed on a shaker for 5 minutes to facilitate breakdown of cell membranes. Protein concentrations were measured using the Pierce BCA protein assay (Thermo Fisher Scientific) with standards prepared in DMEM following the manufacturer's microplate protocol. For plotting of hTLR4 activation, raw values of SEAP production were normalized to protein content obtained with the BCA assay. Mean OD values from untreated cells were subtracted as background from all other normalized values, with resulting values defined as specific activation. The percent specific activation was calculated relative to the maximum activation of TLR4 obtained with 50-nM S100A9.

In one set of experiments aimed to determine activation of TLR4, treatments were prepared with increasing concentrations of S100A9, CAP37, or CAP37-derived peptides. The final concentrations of S100A9 were 1, 5, 10, 50, 100, and 500 nM and 1 µM. The final concentrations of CAP37 were 100, 200, 300, 400, 500, 600, 700, 800, and 900 nM and 1 µM. All peptides were tested at final concentrations of 10 nM, 100 nM, 1 µM, 10 µM, and 100 µM.

In another set of experiments, we determined the effects of CAP37 and peptides on the activation of hTLR4 by S100A9. Experimental treatments were prepared by mixing an equal volume of S100A9 with CAP37 or its peptide. Mixtures were either added to plates immediately before adding cells or pre-incubated for 1 hour at room temperature prior to the addition of cells. In this set of experiments, S100A9 was used at a constant final concentration of 10 nM, which leads to 50% of the maximum TLR4 stimulation. This was to allow us to measure either an increase or a decrease in TLR4 activation in the presence of CAP37 and derived peptides. The final concentrations of CAP37 and peptides were 0.01, 0.1, 1.1, 11, 110, and 550 nM. A positive control of 10-nM S100A9 alone was included in all stimulation assays.

Corneal Abrasion in Mice

This study was carried out in strict accordance with the recommendations in the Guide for the Care and Use of Laboratory Animals of the National Institutes of Health and the ARVO Statement for the Use of Animals in Ophthalmic and Vision Research. The protocol was approved by the Institutional Animal Care and Use Committee of the University of Oklahoma Health Sciences Center (Protocol Number 18-069-I). Corneal abrasion was performed as described before.[13] Briefly, mice (8-week-old female C57BL/6) were anesthetized using ketamine (100 mg/kg) and xylazine (10 ng/kg); to minimize suffering, the systemic analgesic buprenorphine sustained release (ZooPharm, Inc., Laramie, WY, USA) was administered subcutaneously (1 mg/kg) before corneal abrasion was performed. A 2-mm trephine (Integra Miltex, York, PA, USA) was first used to demarcate the cornea of the right eye of the mouse. The corneal epithelium was then removed within the demarcated area using an Algerbrush II (The Alger Companies, Lago Vista, TX, USA).

Immunoblot Analysis of Proteins in Mouse Cornea

Mouse corneas were excised at 0, 2, 4, 6, and 24 hours post-wounding and immediately flash frozen in liquid nitrogen. Corneas were thawed in 200 µl of buffer containing 20-mM Tris-HCl, 150-mM sodium chloride, 1-mM phenylmethylsulfonylfluoride, 0.05% Tween 20, and a 1X Halt Protease Inhibitor Cocktail from Thermo Fisher Scientific. Homogenates were created by disrupting the corneas for 10 minutes at maximum speed in a Bullet Blender (Next Advance, Inc., Averill Park, NY, USA) using 0.9- to 2-mm stainless steel beads. Homogenates were centrifuged at 16,000*g* for 10 minutes to eliminate the froth. Protein concentrations of lysates were determined. Equal amounts of protein (20 µg) from each sample of corneal homogenate were analyzed by electrophoresis on a 12% SDS-PAGE gel and transferred to nitrocellulose membranes (Whatman, Inc., Florham Park, NJ, USA) for western blot analysis. Blots were treated as described previously to quantify S100A9 and β-actin. The mouse monoclonal anti-β-actin primary antibody was from MilliporeSigma (Burlington, MA, USA) and the rabbit polyclonal anti-S100A9 was from Abcam. Blots were analyzed and semiquantified using ImageJ software (National Institutes of Health, Bethesda, MD, USA).

Statistical Analysis

Statistical analysis was performed using GraphPad Prism 7.03 (GraphPad Software, La Jolla, CA, USA). All statistical analyses were performed with a threshold for significance (alpha) set at 0.05. To analyze binding of antigens S100A9 and TLR4/MD-2 to protein or peptide targets, we first subtracted the OD values obtained with 0-nM antigen from the OD values obtained with 10-nM antigen. We then used a one-way ANOVA, followed by Dunnett's multiple comparisons test. For statistical analysis of S100A9 and TLR4/MD-2 dose–response binding, OD values obtained with 0-nM antigen were subtracted as background. We then used a two-way ANOVA, followed by Dunnett's multiple comparisons test. We compared the specific interactions of S100A9 and TLR4/MD-2 antigens with target proteins/peptides with the non-specific interactions of the same antigens with BSA. For TLR4 activation analysis, we used a two-way ANOVA, followed by Dunnett's multiple comparisons test. We compared the percent activation of hTLR4 by S100A9 alone with that of S100A9 combined with increasing concentrations of CAP37 or peptide.

Results

Screening for Interacting Partners of CAP37 in Human Corneal Epithelial Cells

In the current study, a hTCEpi was used with the previously validated TriCEPS-based ligand-receptor glycocapture method[14,16] to identify binding partners of CAP37. This method was chosen because it is designed to identify specific glycosylated receptors expressed on the cell surface through specific ligand-receptor interactions under near physiological conditions in living cultured cells. As shown in Figure 1, among the 45 proteins enriched in the CAP37 samples (log2 of fold change > 0), only seven were more than fourfold enriched in the CAP37 samples compared with the control samples (log2 of fold change > 2). These seven proteins had a statistically significant enrichment in

Investigative Ophthalmology & Visual Science

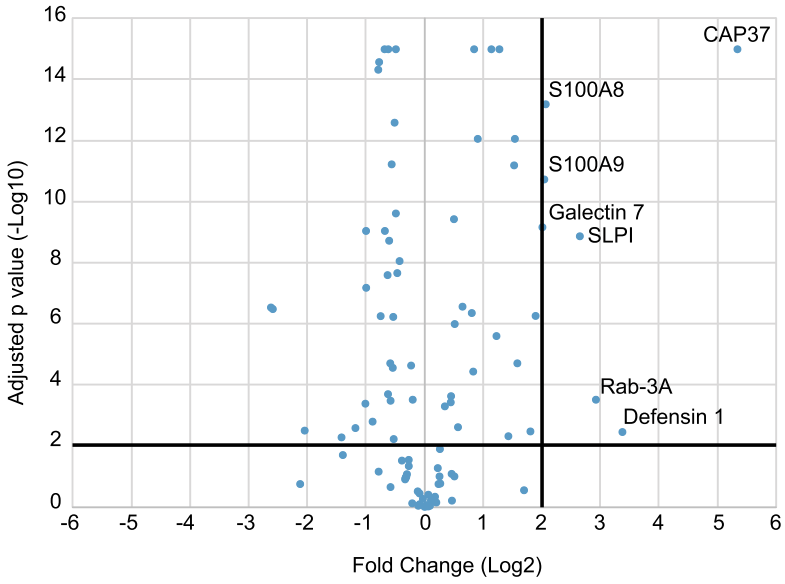

Figure 1. Identification of proteins pulled down by CAP37. Corneal epithelial cells hTCEpi were incubated with TriCEPS conjugated to insulin or CAP37. Cell pellets were analyzed by mass spectrometry at Dualsystems Biotech AG. The resulting volcano plot is shown. Each identified protein is plotted according to its relative abundance in CAP37 versus insulin samples on the *x*-axis (log2 of fold change) and according to its adjusted *P* value on the *y*-axis. The upper right quadrant delimited by the bold lines shows the most significant CAP37-interacting candidates. SLPI, secretory leukocyte protease inhibitor; Rab-3A, Ras-related small GTPase 3A.

Table 1. Significant CAP37-Interacting Partner Candidates

Uniprot Identifier	Protein	Number of Peptides	Log2 Fold Change	Adjusted *P* Value*
P20160	CAP37	7	5.33	1.00E-15
P59665	Defensin 1	2	3.37	0.0034
P20336	Rab-3A	2	2.92	0.0003
P03973	SLPI	7	2.64	1.33E-09
P05109	S100A8	6	2.06	6.33E-14
P06702	S100A9	7	2.04	1.83E-11
P47929	Galectin-7	5	2.00	6.72E-10

**P* values adjusted for multiple comparisons to control the experiment-wide false discovery rate.

the CAP37 samples compared with the control samples. They are plotted above 2 on the *y*-axis (–log10 of adjusted *P* value), which corresponds to an adjusted *P* value of 0.01 or lower. These seven most significant CAP37-interacting partner candidates are listed in Table 1. Surprisingly, none of them is a transmembrane receptor, one (Rab 3A) is an intracellular protein, and six are extracellular proteins. The capture of these proteins by TriCEPS-bound CAP37 suggests that they are able to interact either directly or indirectly with CAP37.

CAP37 Directly Binds to S100A9 In Vitro

We conducted ELISA experiments to test direct binding of CAP37 to the potential interacting partners S100A8 and S100A9, which demonstrated the most significant interaction with CAP37 in the TriCEPS analysis (Fig. 1). A specific, but low, interaction was found between CAP37 and S100A8 (not shown). A much higher specific interaction (at least 10-fold higher) was found between CAP37 and S100A9 (Fig. 2A, black bar). S100A9 was also tested for interaction with its known interacting partner S100A8, which was used as a positive control. Binding of S100A9 to S100A8 (Fig. 2A, open bar) was twofold higher than its binding to CAP37. S100A9 was further tested for interaction with CAP37's most closely related proteins neutrophil elastase (NE) and cathepsin G (CG),[17] but no significant binding was found (Fig. 2A).

As shown in Figure 2B, a dose-dependent interaction was found between CAP37 and increasing concentrations of S100A9. All K_d and B_{max} values obtained in the present study are shown in Table 2. The calculated maximal binding (B_{max}) value of S100A9 was 1.3 (OD value at 492 nm), which reflects the maximum number of binding sites for S100A9 on wells coated with CAP37. The dissociation constant (K_d value), indicating the S100A9 concentration required to reach half-maximal binding at equilibrium, was also calculated. This value was in the low nanomolar range (9.2 nM), which indicates a high affinity of S100A9 for CAP37. In contrast, no interaction was detected between S100A9 and NE or CG, even at the highest concentrations of S100A9. These results suggest that, even though CAP37, NE, and CG have similar

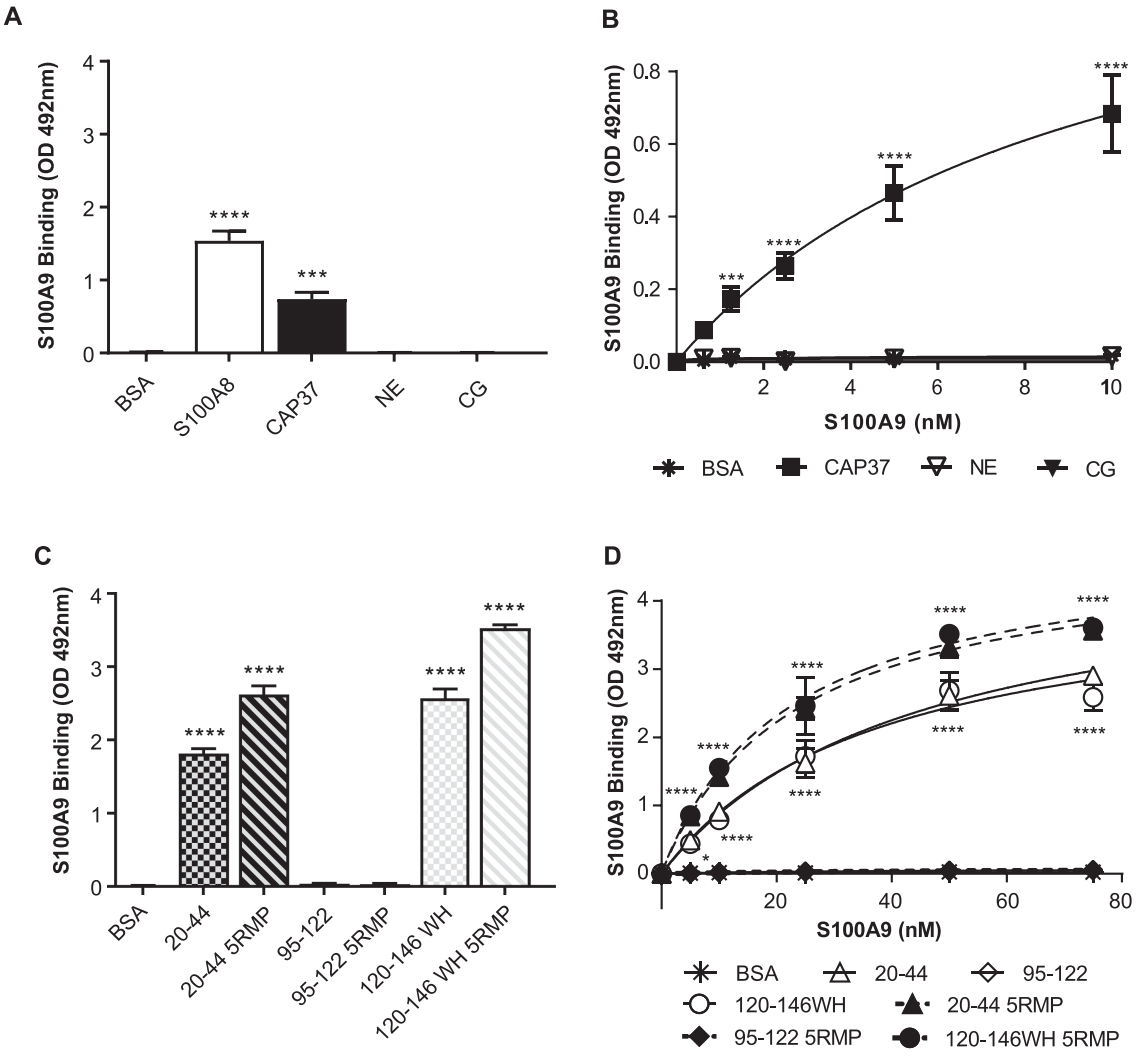

Figure 2. CAP37 and four CAP37-derived peptides directly bind S100A9 in vitro. ELISA plates were coated with the indicated target proteins and peptides. (**A**, **C**) His-tagged S100A9 was added to the coated wells at 0 or 10 nM, and binding was quantified using anti-His tag antibody. Bar graph shows the mean of OD values ± *SEM* from three independent experiments, each done in triplicate. For each experiment, values obtained with 0-nM S100A9 were subtracted as background. A one-way ANOVA followed by Dunnett's multiple comparisons test was used to compare the interaction of S100A9 with each protein (**A**) or peptide (**C**) to the interaction of S100A9 with BSA. Significances of $^{***}P < 0.001$ and $^{****}P < 0.0001$ are shown. (**B**) Binding of increasing concentrations of S100A9 to indicated proteins. Data points are mean ± *SEM* of values obtained from three independent experiments, each done in duplicate. Experimental results were fit to a nonlinear regression curve using GraphPad Prism. For statistical analysis, a two-way ANOVA, followed by Dunnett's multiple comparisons test, was used to compare the interaction of each protein to that of BSA at the same concentration of S100A9. Significances of $^{***}P < 0.001$ and $^{****}P < 0.0001$ are shown. (**D**) Binding of increasing concentrations of S100A9 to the indicated peptides. Results are plotted and analyzed as described in (**B**). Binding of S100A9 to peptides 20-44 and 120-146 WH had significance of $^{*}P < 0.05$ at 5 nM and significance of $^{****}P < 0.0001$ at all tested doses of S100A9 above 5 nM. Binding of S100A9 to peptides 20-44 5R-MP and 120-146 WH 5R-MP had maximum significance ($^{****}P < 0.0001$) at all tested doses of S100A9. Binding of peptides 95-122 and 95-122 5R-MP was not significant at any tested dose of S100A9.

three-dimensional structures, there might be specific, non-overlapping biological effects of CAP37 not exhibited by NE and CG and mediated by a direct and specific interaction between CAP37 and S100A9.

CAP37-Derived Peptides Interact with S100A9 In Vitro

Because our ultimate goal is to develop CAP37-derived peptides for therapeutic use in corneal injuries and infections, we tested six previously described bioactive peptides derived from three different regions of the CAP37 protein. In a previous study, we showed that peptide 95-122, derived from the corresponding sequence of CAP37, could induce migration of corneal epithelial cells,[3] mimicking the effect of the full-length protein.[11,12] As shown previously, this region forms an outer loop at the surface of the native CAP37.[3,18] Thus, we tested whether it could be this region of CAP37 that mediates the interaction with S100A9; however, we found no significant interaction between the CAP37-derived peptide 95-122 and S100A9 (Fig. 2C).

Another peptide, 20-44, derived from the corresponding sequence of CAP37, was also tested for interaction with S100A9. Peptide 20-44 was previously found to have antimicrobial effects,[3,18] mimicking another important biological

Table 2. Binding of CAP37-Derived Peptides to S100A9 and TLR4 and the Effect on TLR4 Activation

Protein/Peptide	K_d/B_{max} S100A9	K_d/B_{max} TLR4/MD-2	Maximum Activation of TLR4 (%)	Maximum Decrease of TLR4 Activation (%)
CAP37	9.2/1.3	98/5	24	5–20
NE	NS	NS	ND	ND
CG	NS	NS	ND	ND
20-44	43.8/4.7	90.6/5.7	15	10–20
20-44 5RMP	23.5/4.7	269.9/10.9	0	15–35
95-122	NS	NS	ND	ND
95-122 5RMP	NS	NS	ND	ND
120-146 WH	37.3/4.3	228.7/8.3	0	10–20
120-146 WH 5RMP	22.3/4.8	18.9/4.4	0	10–15
S100A9	ND	ND	100	0

K_d is shown in nM, B_{max} was OD measured at 492 nm, and activation of TLR4 by a protein or peptide is shown as a percentage relative to the maximum activation of TLR4 by 50-nM S100A9. The maximum decrease from 50% TLR4 activation by 10-nM S100A9 is shown. The first number is from the competition experiments with the protein or peptide, and the second number is from the quenching experiments with protein/peptide. NS, not significant; ND, not determined.

effect of the full-length protein. As shown in Figure 2C, peptide 20-44 interacts strongly with S100A9. As shown in Figure 2D (open triangles), this interaction is dose dependent, similar to that of S100A9 with full-length CAP37 (Fig. 2B). The K_d value is approximately five times higher with this peptide (K_d of 43.8 nM) than with the full-length protein (K_d of 9.2 nM), suggesting a better affinity of S100A9 for the full-length CAP37 than for the peptide 20-44. The B_{max} value is approximately four times higher with this peptide (B_{max} of 4.7) than with the full-length protein (B_{max} of 1.3), suggesting more binding sites for S100A9 in wells coated with 0.5 µg of peptide 20-44 than in wells coated with 0.5 µg of full-length CAP37. This is likely because 0.5 µg contains approximately 10 times more molecules of peptide than protein. As shown in Figure 3, the 20-44 region of CAP37 is mostly buried within the protein, with only a few residues protruding at the surface of CAP37. It is possible, however, that these exposed residues of CAP37 are involved in the binding of S100A9.

We tested another peptide (120-146 WH), also derived from the sequence of CAP37. This peptide was previously found to reproduce the corneal wound-healing effect of the full-length protein, as well as its antimicrobial effect.[13] We found a strong binding of S100A9 to 120-146 WH (Fig. 2C). In Figure 2D (open circles), we show that this interaction is dose dependent, similar to that of S100A9 with full-length CAP37. The K_d value is approximately four times higher with this peptide (K_d of 37.3 nM) than with the full-length protein (K_d of 9.2 nM), suggesting again a better affinity of S100A9 for the full-length CAP37 than for the peptide 120-146 WH. The B_{max} value is approximately three times higher with this peptide (B_{max} of 4.3) than with the full-length protein (B_{max} of 1.3). As previously mentioned, this finding suggests more binding sites for S100A9 in wells coated with the target peptide than in wells coated with the full-length protein. As shown in Figures 4B and 4C, the region of CAP37 between residues 120 and 146 (indicated by blue and yellow) is located both at the surface and internally, buried inside the protein. Figure 4A shows the buried residues (boxed in gray) on the peptide sequence. It is important to note that the bioactive peptide used in this study (120-146 WH) is a modified version of the native 120 to 146 sequence of CAP37 (120-146 QR, shown in Fig. 4).[13] As shown in yellow in Figures 4B and 4C, residues Q131 and R132 are exposed at the surface of CAP37. It is possible that this exposed loop of CAP37 mediates the binding to S100A9 and that the affinity of the native version of S100A9 is different from the affinity of the modified version.

The peptide derivatives 20-44 5RMP, 95-122 5RMP, and 120-146 WH 5RMP were also tested for interaction with S100A9. As shown in Figures 2C and 2D, the addition of 5RMP increases the affinities of S100A9 for peptide 20-44 (K_d of 23.5 vs. 43.8 nM) and peptide 120-146 WH (K_d of 22.3 vs. 37.3 nM). In contrast, peptide derivative 95-122 5RMP still did not interact with S100A9, indicating that the additional R residues and MP moieties are not directly binding S100A9.

CAP37 Directly Binds TLR4/MD-2 In Vitro

In vivo, S100A8 and S100A9 form a heterodimer, named calprotectin in reference to its calcium-binding properties and antimicrobial effects.[19] Calprotectin has high affinity for cell surface molecules, such as heparan sulfate proteoglycans and carboxylated *N*-glycans.[20] S100A8, S100A9, and the calprotectin heterodimer have been described as ligands of receptor for advanced glycation endproducts (RAGE) and TLR4.[20–22] Interestingly, we previously identified RAGE as a direct binding partner and potential receptor for CAP37 and showed that NE and CG could also interact with this receptor.[15,23] Here, we investigated whether CAP37, NE, and CG could interact with TLR4. To perform these in vitro binding experiments, we used a complex between TLR4 and the extracellular protein MD-2, which forms the functional pattern recognition receptor.[24] LPS and S100A8 are known ligands of the TLR4/MD-2 heterodimer and thus served as positive controls.[24,25] Even though S100A9 is also a known ligand of the TLR4/MD-2 heterodimer, we avoided using it as a positive control because the recombinant S100A9 was His-tagged and would have cross-reacted with the anti-His primary antibody used in this experiment to quantify the bound TLR4/MD-2 complex. We found a low, but specific, interaction between CAP37 and the TLR4/MD-2 complex (Fig. 5A, black bar), similar to that of LPS (Fig. 5A, open bar). In contrast, NE and CG did not significantly interact with TLR4/MD-2. These results suggest that CAP37, but not NE or CG, may have specific biological effects mediated by a direct interaction with TLR4. As shown in Figure 5B, there was a dose-dependent interaction between CAP37 and TLR4/MD-2 with a calculated K_d of 98 nM. This finding

Investigative Ophthalmology & Visual Science

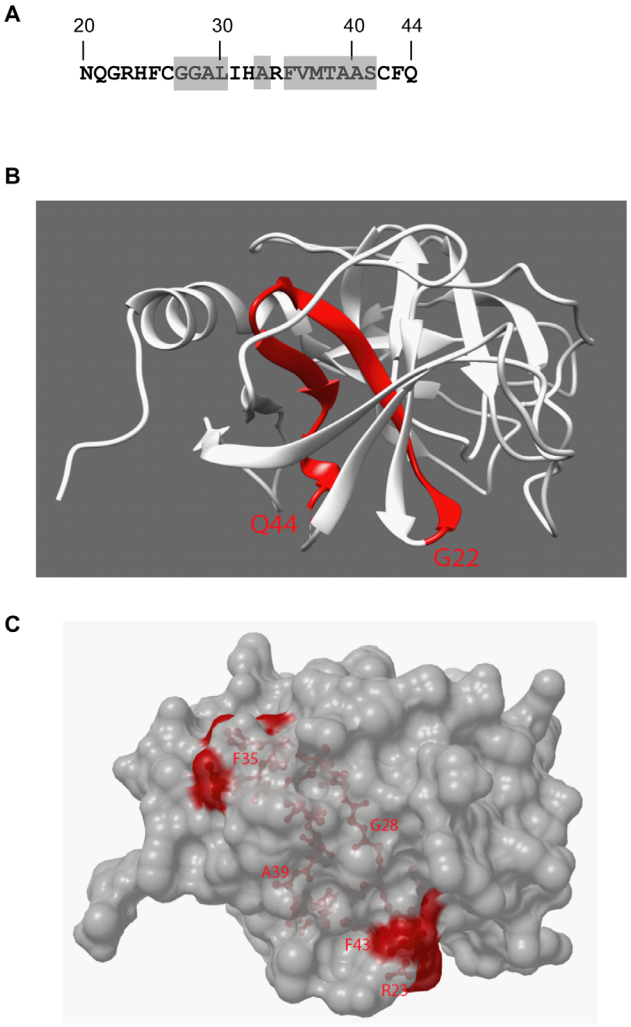

Figure 3. Potential interacting residues within region 20-44 of CAP37. (**A**) The native amino acid sequence of region 20-44 of CAP37 is shown. Shaded residues are nested inside the protein. All other residues are partly or fully exposed at the surface of the protein and could potentially be involved in the interaction with S100A9. (**B**) A ribbon representation of CAP37 made in PYMOL is shown. The 20-44 region is shown in red. It is partly exposed to the surface. (**C**) A surface representation of CAP37 made in PyMOL is shown in the same orientation of the protein shown in (**B**). Small patches of the 20-44 region are exposed at the surface, as shown in red.

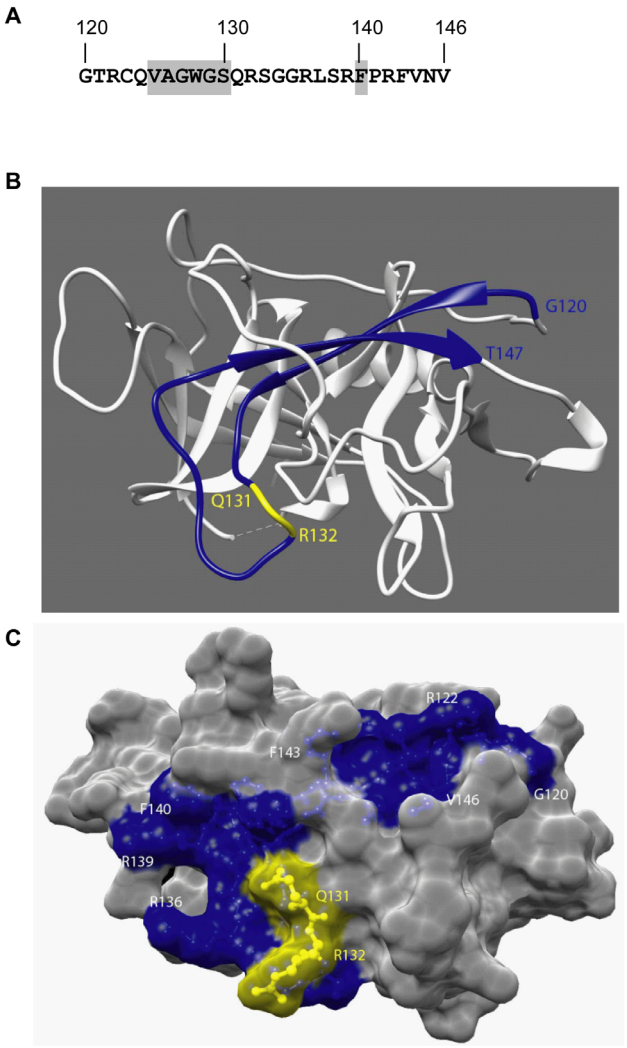

Figure 4. Potential interacting residues within region 120-146 of CAP37. (**A**) The native amino acid sequence of region 120-146 of CAP37 is shown. The shaded residues are nested inside the protein. All other residues are exposed at the surface of the protein. (**B**) A ribbon representation of CAP37 made in PyMOL is shown. The 120-146 region is shown in blue. It is arranged in a hairpin fashion, with two anti-parallel β-sheets that are partly buried and a large loop exposed at the surface. This surface loop contains residues Q131 and R132 (shown in yellow) that have been modified to W131 and H132 in the CAP37-derived peptide described in this study (peptide 120-146 WH). (**C**) A surface representation of CAP37 made in PyMOL is shown in the same orientation of the protein shown in (**B**). The surface loop is indicated in blue and yellow as in (**B**). It is apparent that the first five and last six residues of this region of CAP37 are surface exposed and together form another potential interacting domain in CAP37.

suggests that CAP37 has a ~10-fold lower affinity for TLR4 than for S100A9 (K_d of 9.2 nM).

TLR4/MD-2 Interacts with Peptides 20-44 and 120-146 In Vitro

We also measured interactions of the CAP37-derived peptides with the TLR4/MD-2 complex. Interestingly, the two CAP37-derived peptides found to interact with S100A9 also significantly interacted with TLR4/MD-2 (Fig. 5C). In contrast, peptide 95-122, which did not interact with S100A9, had only minimal interaction with TLR4/MD-2. The addition of 5RMP to these peptides increased the binding of peptide 120-146 WH to TLR4/MD-2. The K_d of TLR4/MD-2 for this peptide changed from 228.7 nM in the absence of 5RMP to 18.9 nM in the presence of 5RMP (Fig. 5D). Peptide 120-146 WH 5RMP has similar affinities for TLR4/MD-2 (K_d of 18.9 nM) and for S100A9 (K_d of 22.3 nM). In contrast, the three other interacting peptides (120-146 WH, 20-44, and 20-44 5RMP) and the full-length CAP37 have stronger affinities for S100A9 than for TLR4/MD-2. Taken together, these results suggest that the administration of any of the four CAP37-derived peptides interacting with S100A9 and TLR4 could mimic the effects of the full-length

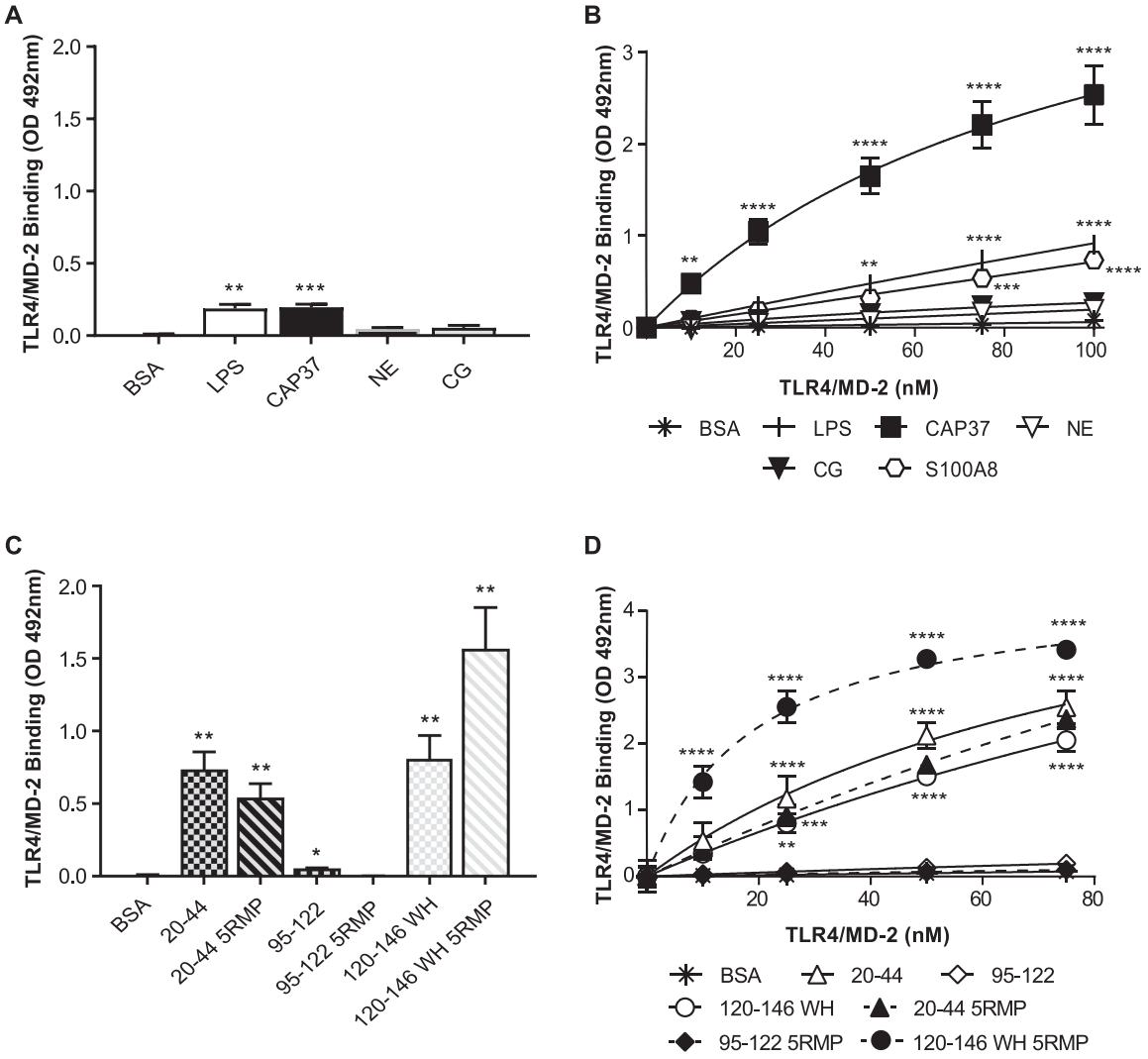

Figure 5. CAP37 and four CAP37-derived peptides directly bind TLR4/MD-2 in vitro. ELISA plates were coated with the indicated proteins and peptides. (**A**, **C**) His-tagged TLR4/MD-2 (at 0 or 10 nM) was added to the coated wells and binding was quantified using anti-His tag antibody. Data are mean ± *SEM* of OD values from three independent experiments, after values with 0-nM TLR4/MD-2 were removed as background. A one-way ANOVA, using Dunnett's multiple comparisons test, compared the binding of each protein (**A**) or peptide (B) to the binding of BSA. Significances of $^{*}P < 0.05$, $^{**}P < 0.01$, and $^{***}P < 0.001$ are shown. (**B**) Dose-dependent binding of TLR4/MD-2 to indicated proteins. Data (mean ± *SEM*) are fitted to a curve of nonlinear regression. A two-way ANOVA was used with Dunnett's multiple comparisons test to compare the binding of each protein to that of BSA at the same concentration of TLR4/MD-2. LPS shows a significant binding of $^{**}P < 0.01$ to TLR4/MD-2 at 50 nM and $^{****}P < 0.0001$ at all higher doses. CAP37 shows significance with $^{**}P < 0.01$ at 10 nM and $^{****}P < 0.0001$ at all higher doses of TLR4/MD-2. S100A8 showed significant binding to TLR4/MD-2 at 75 nM ($^{***}P < 0.001$) and at 100 nM ($^{****}P < 0.0001$). Binding of NE and CG was not significant. (**D**) Dose-dependent binding of TLR4/MD-2 to peptides. Results are plotted and analyzed as described in (**B**). At all tested doses of TLR4/MD-2, the binding of peptide 120-146WH 5R-MP showed maximum significance of $^{****}P < 0.0001$. Peptides 20-44, 20-44 5R-MP, and 120-146WH significantly bind TLR4/MD-2 at 25 nM and reach maximum significance ($^{****}P < 0.0001$) at 50 nM. Binding of peptides 95-122 and 95-122 5R-MP was not significant at any tested dose.

CAP37 on the cornea by disrupting the binding of endogenous S100A9 and/or calprotectin to TLR4.

CAP37 and Peptide 20-44 Are Partial Agonists of TLR4

To explore the significance of these newly identified CAP37 ligands of TLR4, we measured their abilities to activate this receptor as agonists in HEK-hTLR4 cells. In this experiment, we used S100A9 as a positive control because it is a known agonist of TLR4. As shown in Figure 6A, a dose-dependent activation of TLR4 was obtained with S100A9, with the maximal stimulation of the receptor obtained with 50-nM (5×10^{-8} M) S100A9, and half-maximal stimulation when using ~10-nM (10^{-8} M) S100A9 (both indicated by the dotted lines). In contrast, CAP37 only began to activate TLR4 receptor at 100 nM (10^{-7} M). This activation was dose dependent between 100 nM and 1 µM (10^{-6} M), which was the highest tested dose of CAP37. CAP37 could only partly activate TLR4, up to 24% of the maximal activation by S100A9, when used at 1 µM (Fig. 6A, first arrow). This suggests that CAP37 is a partial agonist of the TLR4 receptor, which begins to activate TLR4 at a concentration that is approximately 100-fold

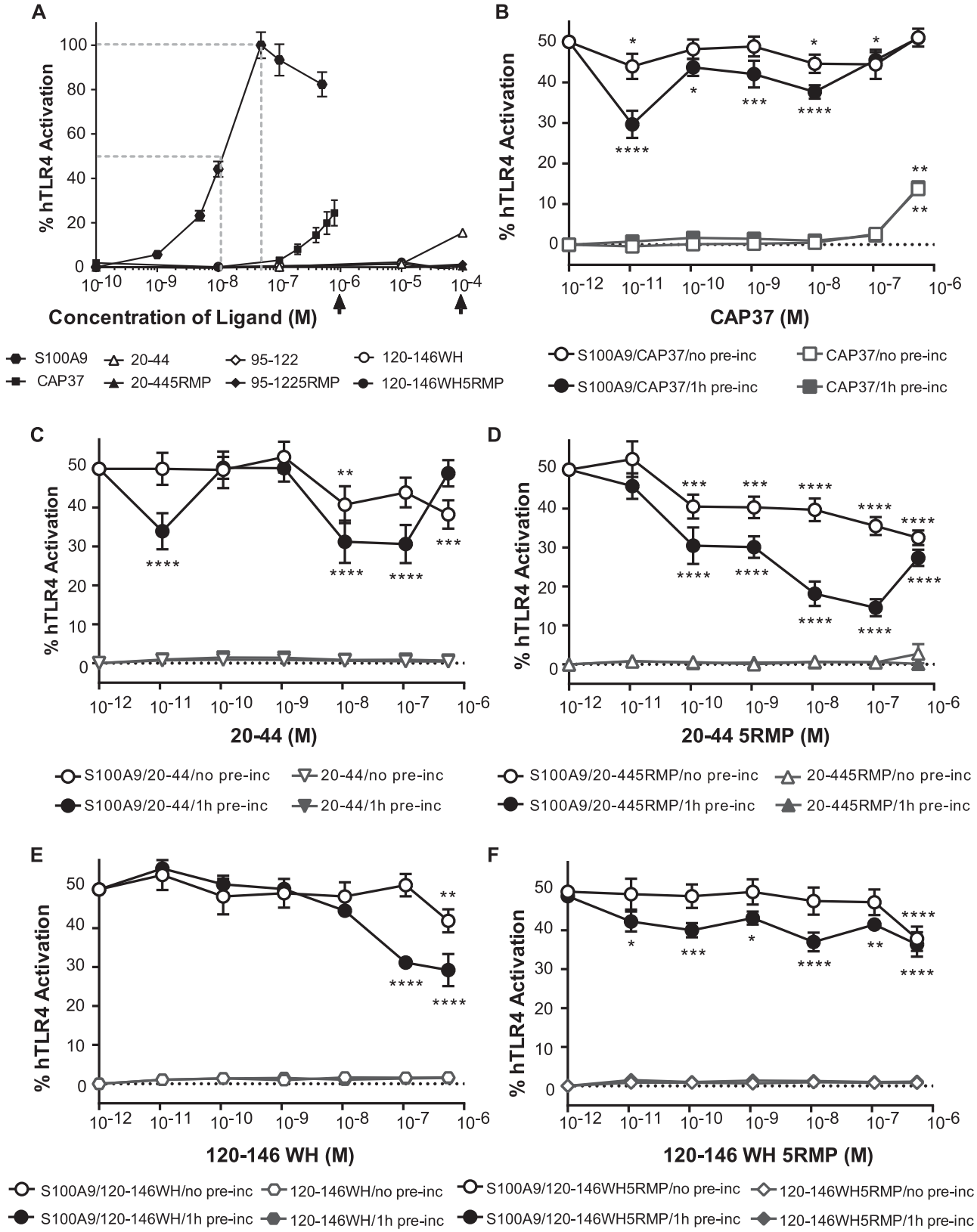

Figure 6. Effects of CAP37 and CAP37-derived peptides on TLR4. (**A**) CAP37 and peptide 20-44 are partial agonists of TLR4. The ability of increasing concentrations of S100A9, CAP37, and CAP37-derived peptides to stimulate TLR4 was measured in HEK-hTLR4 cells. SEAP production in cell medium was measured following 24-hour incubation with ligands. Data shown are mean percent activation ± *SEM* relative to activation induced by S100A9 at 50 nM, arbitrarily defined as 100%. Results are from three experiments, each done in triplicate. First arrow, partial activation of TLR4 by CAP37; second arrow, partial activation of TLR4 by peptide 20-44. (**B–F**) Inhibitory effects of CAP37

protein and peptides on the activation of TLR4 by S100A9. Cells were treated with S100A9 at 10 nM alone or in combination with increasing concentrations of CAP37 (**B**) or CAP37 peptides (**C–F**). Filled symbols denote preincubation of CAP37 or the indicated peptide with 0- or 10-nM S100A9 for 1 hour before treatment. Open symbols denote co-treatment with 0- or 10-nM S100A9 without preincubation before treatment. Following 24-hour treatment, SEAP production was quantified. Results show the 50% activation of TLR4, induced by 10-nM S100A9 alone, and activations below 50% with indicated concentrations of CAP37 or CAP37 peptides. Data shown are mean ± *SEM* from three experiments, each done in triplicate. A two-way ANOVA, followed by Dunnett's multiple comparisons test, compared the percent activation of hTLR4 by S100A9 alone with that of S100A9 combined with CAP37 or peptide. Statistical significances of inhibitions are indicated on the graphs as follows: $^{*}P < 0.05$; $^{**}P < 0.01$; $^{***}P < 0.001$; and $^{****}P < 0.0001$.

higher than that of the agonist S100A9. We also found a small partial activation of TLR4 with peptide 20-44, up to 15% of the maximal activation by S100A9, at the highest tested dose of 100 µM (10^{-4} M) (Fig. 6A, second arrow). Peptide 20-44 appears to be a partial agonist that begins activating TLR4 at a concentration that is 100-fold higher than that of the full-length CAP37. None of the other CAP37-derived peptides could activate TLR4, even at the highest tested dose of 100 µM. These results are summarized in Table 2, fourth column. Because CAP37 and the CAP37-derived ligands of TLR4 are either partial agonists or non-agonists, we hypothesized that they could exert an antagonistic effect on TLR4 activation.

CAP37 Has Antagonistic/Inhibitory Effects on the Activation of TLR4 by S100A9

To determine whether the binding of CAP37 to S100A9 and/or TLR4 could modulate (inhibit or potentiate) the activation of TLR4 by S100A9, we measured the activation of this receptor in HEK-hTLR4 cells treated with a 10-nM fixed concentration of S100A9, leading to 50% stimulation of TLR4 in the presence of increasing concentrations of CAP37. One set of co-treatments with S100A9 and CAP37 was preincubated for an hour to promote interaction between the two ligands, prior to addition to the HEK-hTLR4 cells (Fig. 6B, black circles). This set was designed to determine whether the binding of CAP37 to S100A9 inhibits the activation of TLR4 by S100A9 through a quenching mechanism. A second set of co-treatments was prepared by mixing the two proteins immediately before addition to the cells (Fig. 6B, open circles). This set was designed to determine whether CAP37 might be competing with S100A9 for the same binding site on TLR4.

As shown in Figure 6B (open circles), in the absence of preincubation, a modest but significant competitive inhibition of S100A9 was found. In this set of co-treatments, the activation of TLR4 by 10-nM S100A9 remained close to 50% when CAP37 was present at increasing concentrations from 0.01 nM (10^{-11} M) to 1 µM (10^{-6} M). A more significant inhibition of the effect of S100A9 was found when CAP37 was preincubated with S100A9, as shown in Figure 6B (black circles). Surprisingly, this inhibition does not appear to be directly correlated with the concentrations of CAP37. In fact, lower concentrations of CAP37 appear to inhibit more than do the higher concentrations. CAP37 used at 0.01 nM (10^{-11} M) led to an ~20% decrease of TLR4 activation (from 50% to 30%), whereas 10-nM (10^{-8} M) CAP37 led to only a 10% decrease, and 1-µM (10^{-6} M) CAP37 produced no decrease of TLR4 activation. As shown in Figure 6A, CAP37 by itself can partially activate TLR4 beginning at 100 nM (10^{-7} M). This might explain the loss of inhibition when CAP37 concentrations are above 100 nM. Importantly, even the highest concentration of CAP37 does not significantly increase the activation of TLR4 by S100A9, suggesting that there are no additive or synergistic effects of CAP37 and S100A9 on TLR4 activation.

Taken together, these results indicate that low concentrations of CAP37 can mediate partial inhibition of the effect of S100A9 on TLR4 activation and that this inhibitory effect is lost at higher concentrations of CAP37.

Peptides 20-44 and 120-146 Have Antagonistic/Inhibitory Effects on the Activation of TLR4 by S100A9

The CAP37-derived peptides competitively inhibit the activation of TLR4 by S100A9 (Figs. 6C–6F, open circles) in a dose-dependent fashion more significantly than CAP37 (Fig. 6B, open circles). However, inhibitions remain partial, resulting in no more than a 15% decrease of TLR4 activation by S100A9 (results summarized in Table 2, first number in last column). The maximum inhibition mediated by each peptide does not appear to be directly correlated with the affinities of these peptides for TLR4 (Table 2, third column). More information about the binding site of these peptides on TLR4 will be needed to interpret these results and determine whether these are true competitive inhibitions of the TLR4 activation by S100A9 or whether an allosteric inhibition of the receptor might be taking place.

When the quenching of S100A9 is allowed by preincubation with peptides, the inhibitory effects of peptides are generally stronger (Figs. 6C–6F, black circles), similar to the results obtained with CAP37 (Fig. 6B, black circles). This might be because CAP37 and the peptides have more affinity for S100A9 than they do for TLR4. However, once again, the quenching effects mediated by peptides (summarized in Table 2, second number in last column) do not appear to be correlated with the respective affinities of these peptides for S100A9 (Table 2, second column). As seen with CAP37, the inhibitory effects of peptides are not always directly correlated with the concentrations of the peptides. More information on the mechanism and stoichiometry of these interactions will be needed to interpret these results.

The general conclusion from these experiments is that CAP37 and the CAP37-derived peptides that can significantly bind both S100A9 and TLR4 are leading to partial but significant inhibition of TLR4 activation by S100A9. This inhibition seems to be mediated more prominently by a quenching effect on S100A9 than through a direct binding to the TLR4 receptor.

The S100A9 protein is upregulated following corneal abrasion

To our knowledge, the role of S100A9 in corneal epithelial wound healing has not been previously studied. We investigated if the S100A9 protein was expressed in mouse cornea following epithelial abrasion. As shown in

Investigative Ophthalmology & Visual Science

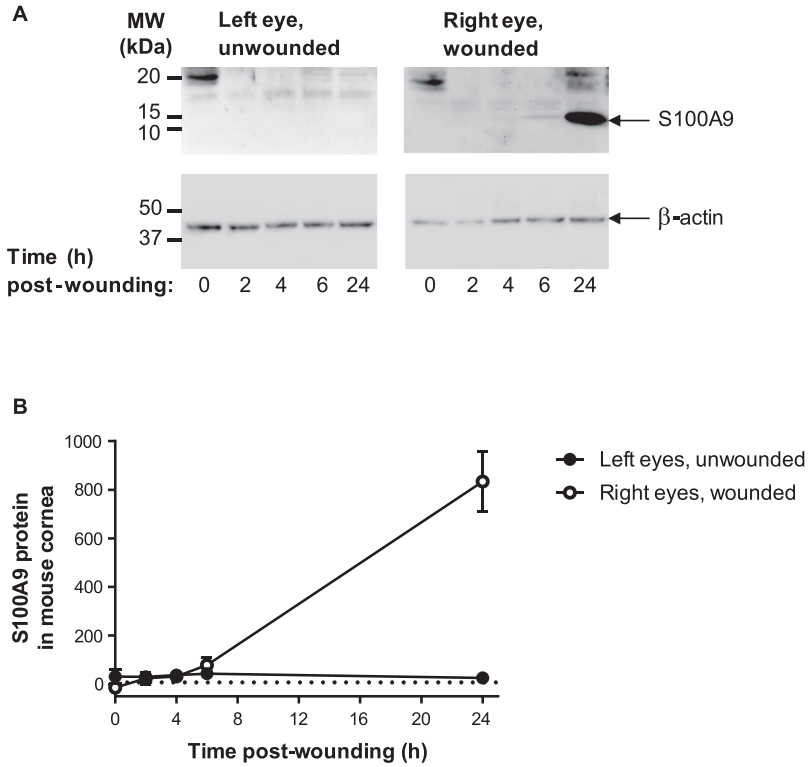

Figure 7. S100A9 protein is upregulated in abraded mouse cornea. (**A**) Corneas from the right eyes were abraded and left eyes were left unwounded. Corneas were dissected at indicated post-wounding times, and extracted proteins were analyzed by immunoblot to quantify S100A9 protein and β-actin. Representative immunoblot from one experiment is shown. (**B**) S100A9 signals from three independent experiments were quantified and normalized to β-actin and are shown as mean $\pm$ *SEM*, in arbitrary units.

Figure 7, corneal S100A9 is undetectable by western blot between 0 and 4 hours post-wounding and then increases between 6 and 24 hours post-wounding in abraded mouse corneas. S100A8 and S100A9 are known to be expressed and released by corneal epithelial cells.[9,26,27] These proteins are also constitutively expressed in neutrophils, where they represent about 40% of all cytosolic proteins. The increase of S100A9 protein correlates with the peak of neutrophil infiltration in the stroma that takes place at 12 to 18 hours post-wounding,[8] suggesting that the detected corneal S100A9 could be of neutrophil origin.[28] A careful investigation of the spatiotemporal expression of S100A9 following corneal abrasion will be necessary to estimate the contribution of the epithelial versus neutrophil origins of S100A9 in the cornea. The increase of S100A9 protein in the cornea between 6 and 24 hours post-wounding establishes that this protein can be a target for treatments with CAP37-derived peptides.

Discussion

Corneal abrasion induces local inflammation, as evidenced by the infiltration of neutrophils in the corneal stroma and the release of cytokines and chemokines.[8,29] Early activation of the innate immune system and inflammatory response is important to ensure efficient healing and protection against invading pathogens.[30] However, uncontrolled inflammation of the cornea is detrimental because it can lead to sight-threatening damage to the cornea, such as scarring, melting, or ulceration.[30]

The current study identified S100A9 as a direct binding partner of CAP37 and CAP37-derived peptides, and, as shown in Figure 7, S100A9 is upregulated in the cornea, following corneal abrasion. When it has been released into the extracellular environment, S100A9 mediates inflammation and protects against invading pathogens. S100A8 and S100A9 proteins are defined as damage-associated molecular patterns and exert their proinflammatory effects through the engagement of pattern recognition receptors, such as TLR4 and RAGE.[31]

In recent studies, a role for TLR4 and RAGE in corneal epithelial wound healing has been reported.[32,33] A functional TLR4/MD-2 complex becomes detectable by western blot in the mouse corneal epithelium as early as 2 hours post-wounding, peaks at 6 hours after wounding, and then gradually returns to baseline by 24 hours.[32] An *in vitro* scratch assay on human corneal epithelial cells showed that the addition of LPS to activate TLR4 at 6 hours post-scratching increased in vitro wound closure, measured at 10 hours.[32] This finding suggests that an early activation of TLR4 could promote corneal epithelial wound healing. RAGE expression is already detectable in the cornea before wounding and was found to be increased at 24 hours post-wounding. RAGE knockout mice had a significant delay in re-epithelialization at 24 and 48 hours post-wounding.[33] Taken together, these results suggest that both receptors support corneal re-epithelialization.

We posit that proper initiation and then resolution of TLR4- and RAGE-mediated immune responses are required to promote corneal re-epithelialization. Our current study suggests that CAP37 and several CAP37-derived peptides could inhibit, rather than activate, the S100A9/TLR4 pathway at the ocular surface. This inhibition may be important

for the resolution of TLR4 activation, which might otherwise become detrimental to the cornea. In our previous studies, we applied CAP37 and peptide 120-146 WH treatments at 0 and 16 hours post-wounding.[6,13] The 0-hour treatment most likely did not have an effect on the S100A9/TLR4 pathway because these proteins are not detectable in the cornea at this time (Fig. 7).[32] Therefore, we believe that the effect of treatments applied at the 0 hour and resulting in the 10% to 15% increase in wound closure measured at 16 hours is mediated by another mechanism.[6,13] This early effect may be mediated by a GPCR and/or activation of PKCδ, as suggested by our previous studies.[6,12] The 16-hour treatment, on the other hand, could have an effect on S100A9 and on the S100A9/TLR4 pathway because both proteins are detectable in the cornea at this time (Fig. 7).[32] In another previous study, we investigated the cytokine response to corneal abrasion, in the absence and presence of CAP37 topical treatments applied at 0 and 16 hours post-wounding.[29] Interestingly, we found that at 24 hours post-wounding, several cytokines and chemokines significantly induced by corneal abrasion, namely RANTES (CCL5), IL-15, MIG (CXCL9), KC (CXCL1), TNF-α, and IL-10, were significantly downregulated by the treatment with CAP37 when compared with vehicle control.[29] This is leading us to hypothesize that activation of TLR4 by S100A9 could have been inhibited by the CAP37 treatment administered at 16 hours post-wounding. This inhibition would in turn lead to a decrease in NF-κB activation by TLR4 and the significant downregulation of cytokines and chemokines. It is unknown whether such inhibition would be able to mediate the 10% to 15% increase in re-epithelialization measured at 24 hours in the eyes treated with CAP37 and peptide 120-146 WH,[6,13] but it is conceivable that at this later time point inhibition rather than activation of TLR4 would enhance wound closure. The hypothesis that CAP37-derived peptides can inhibit the S100A9/TLR4 pathway, thus inhibiting corneal inflammation and possibly activating corneal wound healing, will have to be tested in future in vivo studies.

Inhibition of the S100A9/TLR4 pathway by CAP37-derived peptides, if established in vivo, could have additional benefits at the ocular surface, beyond corneal re-epithelialization. Elevated expression of S100A8 and S100A9 in the cornea has been correlated with inflammation, infection, and neovascularization.[19,28] For example, the expression levels of S100A8 and S100A9 are greatly induced in Gram-positive and Gram-negative induced bacterial keratitis.[34,35] Further, the knockdown of S100A8/S100A9 was found to decrease corneal inflammation and corneal perforation.[34] These studies suggest that inhibition of molecular targets S100A8/S100A9 could be beneficial for better preservation and healing of the cornea during bacterial keratitis resolution. We believe that a CAP37-derived peptide that could inhibit the S100A9/TLR4 signaling while killing the invading bacteria at the same time would be beneficial for therapeutic use in corneal injuries and infections.

Acknowledgments

The authors thank Simon Terzyan and the Laboratory of Biomolecular Structure and Function core facility for assistance with the generation of Figures 3 and 4; Paul Helbling and his team at Dualsystems Biotech for their guidance with the LRC-TriCEPS experiment and for the identification of candidates by LC-MS/MS; Mark Dittmar and the Live Animal Imaging and Functional Analysis core facility for assistance with the animal experiments; Stephen Neely for assistance with the statistical analysis of the results; and Kathy J. Kyler for reviewing this manuscript.

Supported in part by National Institutes of Health National Eye Institute Grants R21EY026229 and P30EY021725 and National Institute of General Medical Sciences Grants P20GM103640 and U54GM104938; Oklahoma Center for the Advancement of Science and Technology Grant HR15-108; and a seed Grant and funds from the Herbert and Dorothy Langsam Chair in Geriatric Pharmacy from the College of Pharmacy at the University of Oklahoma Health Sciences Center.

Disclosure: **A. Kasus-Jacobi**, Biolytx Pharmaceuticals Corp. (F), P; **C.A. Land**, None; **A.J. Stock**, None; **J.L. Washburn**, None; **H.A. Pereira**, Biolytx Pharmaceuticals Corp. (F, I), P

References

1. Domingo E, Zabbo CP. *Corneal Abrasion*. Treasure Island, FL: StatPearls Publishing; 2020.
2. Wipperman JL, Dorsch JN. Evaluation and management of corneal abrasions. *Am Fam Physician*. 2013;87:114–120.
3. Griffith GL, Kasus-Jacobi A, Pereira HA. Bioactive antimicrobial peptides as therapeutics for corneal wounds and infections. *Adv Wound Care (New Rochelle)*. 2017;6:175–190.
4. Dua HS, Gomes JA, Singh A. Corneal epithelial wound healing. *Br J Ophthalmol*. 1994;78:401–408.
5. Ziaei M, Greene C, Green CR. Wound healing in the eye: therapeutic prospects. *Adv Drug Deliv Rev*. 2018;126:162–176.
6. Griffith GL, Kasus-Jacobi A, Lerner MR, Pereira HA. Corneal wound healing, a newly identified function of CAP37, is mediated by protein kinase C delta (PKCδ). *Invest Ophthalmol Vis Sci*. 2014;55:4886–4895.
7. Pereira HA. CAP37, a neutrophil-derived multifunctional inflammatory mediator. *J Leukoc Biol*. 1995;57:805–812.
8. Li Z, Burns AR, Smith CW. Two waves of neutrophil emigration in response to corneal epithelial abrasion: distinct adhesion molecule requirements. *Invest Ophthalmol Vis Sci*. 2006;47:1947–1955.
9. Ruan X, Chodosh J, Callegan MC, et al. Corneal expression of the inflammatory mediator CAP37. *Invest Ophthalmol Vis Sci*. 2002;43:1414–1421.
10. Liu CY, Kao WW. Corneal epithelial wound healing. *Prog Mol Biol Transl Sci*. 2015;134:61–71.
11. Pereira HA, Ruan X, Gonzalez ML, Tsyshevskaya-Hoover I, Chodosh J. Modulation of corneal epithelial cell functions by the neutrophil-derived inflammatory mediator CAP37. *Invest Ophthalmol Vis Sci*. 2004;45:4284–4292.
12. Griffith GL, Russell RA, Kasus-Jacobi A, et al. CAP37 activation of PKC promotes human corneal epithelial cell chemotaxis. *Invest Ophthalmol Vis Sci*. 2013;54:6712–6723.
13. Kasus-Jacobi A, Noor-Mohammadi S, Griffith GL, Hinsley H, Mathias L, Pereira HA. A multifunctional peptide based on the neutrophil immune defense molecule, CAP37, has antibacterial and wound-healing properties. *J Leukoc Biol*. 2015;97:341–350.
14. Frei AP, Moest H, Novy K, Wollscheid B. Ligand-based receptor identification on living cells and tissues using TRICEPS. *Nat Protoc*. 2013;8:1321–1336.
15. Stock AJ, Kasus-Jacobi A, Wren JD, Sjoelund VH, Prestwich GD, Pereira HA. The role of neutrophil proteins on the amyloid beta-RAGE axis. *PLoS One*. 2016;11:e0163330.
16. Frei AP, Jeon OY, Kilcher S, et al. Direct identification of ligand-receptor interactions on living cells and tissues. *Nat Biotechnol*. 2012;30:997–1001.

17. Iversen LF, Kastrup JS, Bjorn SE, et al. Structure of HBP, a multifunctional protein with a serine proteinase fold. *Nat Struct Biol*. 1997;4:265–268.
18. Pereira HA, Erdem I, Pohl J, Spitznagel JK. Synthetic bactericidal peptide based on CAP37: a 37-kDa human neutrophil granule-associated cationic antimicrobial protein chemotactic for monocytes. *Proc Natl Acad Sci U S A*. 1993;90:4733–4737.
19. Tong L, Lan W, Lim RR, Chaurasia SS. S100A proteins as molecular targets in the ocular surface inflammatory diseases. *Ocul Surf*. 2014;12:23–31.
20. Shabani F, Farasat A, Mahdavi M, Gheibi N. Calprotectin (S100A8/S100A9): a key protein between inflammation and cancer. *Inflamm Res*. 2018;67:801–812.
21. Wu R, Duan L, Cui F, et al. S100A9 promotes human hepatocellular carcinoma cell growth and invasion through RAGE-mediated ERK1/2 and p38 MAPK pathways. *Exp Cell Res*. 2015;334:228–238.
22. Laouedj M, Tardif MR, Gil L, et al. S100A9 induces differentiation of acute myeloid leukemia cells through TLR4. *Blood*. 2017;129:1980–1990.
23. Stock AJ, Kasus-Jacobi A, Pereira HA. The role of neutrophil granule proteins in neuroinflammation and Alzheimer's disease. *J Neuroinflammation*. 2018;15:240.
24. Chen L, Fu W, Zheng L, Wang Y, Liang G. Recent progress in the discovery of myeloid differentiation 2 (MD2) modulators for inflammatory diseases. *Drug Discov Today*. 2018;23:1187–1202.
25. Vogl T, Tenbrock K, Ludwig S, et al. Mrp8 and Mrp14 are endogenous activators of Toll-like receptor 4, promoting lethal, endotoxin-induced shock. *Nat Med*. 2007;13:1042–1049.
26. Benito MJ, Calder V, Corrales RM, et al. Effect of TGF-beta on ocular surface epithelial cells. *Exp Eye Res*. 2013;107:88–100.
27. Li J, Riau AK, Setiawan M, et al. S100A expression in normal corneal-limbal epithelial cells and ocular surface squamous cell carcinoma tissue. *Mol Vis*. 2011;17:2263–2271.
28. Schenten V, Plancon S, Jung N, et al. Secretion of the phosphorylated form of S100A9 from neutrophils is essential for the proinflammatory functions of extracellular S100A8/A9. *Front Immunol*. 2018;9:447.
29. Kasus-Jacobi A, Griffith GL, Lerner M, Pereira HA. Effect of cationic antimicrobial protein CAP37 on cytokine profile during corneal wound healing. *J Ocul Dis Ther*. 2017;5:19–27.
30. Ueta M, Kinoshita S. Ocular surface inflammation is regulated by innate immunity. *Prog Retin Eye Res*. 2012;31:551–575.
31. Leanderson T, Liberg D, Ivars F. S100A9 as a pharmacological target molecule in inflammation and cancer. *Endocr Metab Immune Disord Drug Targets*. 2015;15:97–104.
32. Eslani M, Movahedan A, Afsharkhamseh N, Sroussi H, Djalilian AR. The role of Toll-like receptor 4 in corneal epithelial wound healing. *Invest Ophthalmol Vis Sci*. 2014;55:6108–6115.
33. Nass N, Trau S, Paulsen F, Kaiser D, Kalinski T, Sel S. The receptor for advanced glycation end products RAGE is involved in corneal healing. *Ann Anat*. 2017;211:13–20.
34. Deng Q, Sun M, Yang K, et al. MRP8/14 enhances corneal susceptibility to *Pseudomonas aeruginosa* infection by amplifying inflammatory responses. *Invest Ophthalmol Vis Sci*. 2013;54:1227–1234.
35. Roy S, Marla S, Praneetha DC. Recognition of *Corynebacterium pseudodiphtheriticum* by Toll-like receptors and up-regulation of antimicrobial peptides in human corneal epithelial cells. *Virulence*. 2015;6:716–721.